JAIST Repository
https://dspace.jaist.ac.jp/

Title	Crystallization of electron beam evaporated a-Si films on textured glass substrates by flash lamp annealing
Author(s)	Kurata, Keisuke; Ohdaira, Keisuke
Citation	Japanese Journal of Applied Physics, 58(SB): SBBF10-1-SBBF10-5
Issue Date	2019-03-05
Type	Journal Article
Text version	author
URL	http://hdl.handle.net/10119/16220
Rights	This is the author's version of the work. It is posted here by permission of The Japan Society of Applied Physics. Copyright (C) 2019 The Japan Society of Applied Physics. Keisuke Kurata and Keisuke Ohdaira, Japanese Journal of Applied Physics, 58(SB), 2019, SBBF10-1-SBBF10-5. http://dx.doi.org/10.7567/1347-4065/aafb51
Description	

JAIST
JAPAN ADVANCED INSTITUTE OF SCIENCE AND TECHNOLOGY

Japan Advanced Institute of Science and Technology

Crystallization of electron-beam evaporated a-Si films on textured glass substrates by flash lamp annealing

Keisuke Kurata and Keisuke Ohdaira

Japan Advanced Institute of Science and Technology, Nomi, Ishikawa, 923-1292, Japan

*E-mail: *ohdaira@jaist.ac.jp*

We investigate the crystallization of amorphous silicon (a-Si) films, by flash lamp annealing (FLA), formed by electron beam (EB) evaporation on textured glass substrates. We confirmed that EB-evaporated a-Si films formed on textured glass can be crystallized by FLA. Optical reflectance on EB-evaporated a-Si can be reduced by using the texture glass, leading to a reduction in the fluence of a FL pulse required for the crystallization. The fluence of a FL pulse for the crystallization of EB-evaporated a-Si films tends to increase with temperature during the EB evaporation of a-Si films. The pre-existing crystal grains in precursor Si films may affect the mechanism of their crystallization. The usage of textured glass substrates leads the formation of polycrystalline Si (poly-Si) films with fine grains. This may results from the prevention of lateral thermal growth and the suppression of explosive crystallization (EC). Unlike in the case of the crystallization of EB-evaporated a-Si films on flat glass substrates, poly-Si films formed on textured glass substrates are not cracked. This may be due to the change in the suppression of the emergence of EC.

1. Introduction

In recent years, renewable energy such as solar cells has attracted much attention. Solar cells are a power generation method using sunlight that lasts semipermanently and has attracted attention as a clean power generation method that does not require fossil fuel exhaustion. Among many types of solar cells, crystalline Si (c-Si) solar cells using Si wafers have been widely used and dominated the present photovoltaic (PV) market. However, for further reduction in the cost of PV modules, decrease in the usage of Si material is desired. Solar cells consisting of thin-film Si can reduce the consumption of Si material compared to those with Si wafers. Amorphous Si (a-Si) and microcrystalline Si (μc-Si) had been intensively investigated. μc-Si thin films has a difficulty of controlling the film uniformity in a large-area wafer, and a-Si shows photo-induced degradation by which its performance deteriorates markedly with the duration of exposure to sunlight.

Thin-film polycrystalline (poly-Si) solar cells formed on low-cost substrates, such as glass substrates, have been receiving attention as next-generation solar cells because of low material usage as well as high stability against light soaking.[1–9] In recent years, researches have been conducted to crystallize an a-Si thin film by annealing to form poly-Si thin films. Short-time annealing methods have been widely used for the crystallization of a-Si films because of high productivity[10–23]. In the short-time annealing methods, heating duration is one of the most important factors for the crystallization of thick a-Si films and the suppression of thermal damage to substrates. Rapid thermal annealing (RTA) has an annealing duration of >1 s, leading to the heating of entire substrates along the depth. On the contrary, excimer laser annealing (ELA) cannot crystallize a-Si films on the order of several μm, which is needed for solar cell application, due to insufficient annealing duration.

Flash lamp annealing (FLA) is an annealing method using millisecond-order discharge light from Xe lamps.[24–26] The millisecond-order annealing duration results in a thermal diffusion length of several tens of μm in a-Si and glass. The proper thermal diffusion length enables the crystallization of μm-order-thick a-Si films with no serious thermal damage to entire glass substrates. We have thus far clarified that the crystallization of a-Si films by FLA takes place laterally based on a mechanism referred to as explosive crystallization (EC).[27] The schematic diagram of EC is shown in Fig. 1. EC is based on heat generation due to enthalpy difference between metastable a-Si and stable c-Si phases and its diffusion to

surrounding a-Si. In particular, when an Electron-beam- (EB-) evaporated a-Si film is used as a precursor, EC based on liquid-phase epitaxy occurs, and a poly-Si film composed of large grains can be formed. Since the EB-evaporated a-Si films, formed under ultra-high vacuum, contains only small amount of impurities, their crystallization is more difficult to be triggered than the cases for other precursor a-Si films formed by different deposition methods such as catalytic chemical vapor deposition and sputtering. A FL pulse light with higher fluence is thus required for the crystallization of EB-evaporated a-Si films. Another issue for the crystallization of EB-evaporated a-Si films is the cracking of Si films during the crystallization, which is partly due to the inherent tensile stress of EB-evaporated a-Si films. [28–31]

To solve these problems, in this study, we attempted to use textured glass for the substrates of EB-evaporated a-Si films. An antireflection effect and resulting increase in the optical path length are expected by using textured glass substrates, which can contribute to a reduction in a fluence of FL pulse needed for crystallization.[32] We also clarify the effect of using textured glass substrates on the crystallization mechanism of EB-evaporated a-Si films and on the suppression of cracking in poly-Si films. Furthermore, the influence of the substrate temperature during EB evaporation is also investigated.

2. Experimental methods

We first cleaned 19.8 mm × 19.8 mm-sized flat Eagle XG glass substrates ultrasonically in acetone, ethanol, and de-ionized water for 5 minutes, respectively. Reactive ion etching (RIE) was performed on the surface of the glass substrates to form textured structures. We systematically changed RIE duration to control the roughness of the glass surfaces. The RIE of glass surfaces was performed using CF_4 at a pressure of 2.6 Pa and a RF power of 200 W for 0–3 hours. The surface roughness of the glass substrates was evaluated by atomic force microscopy (AFM). Figure 2 shows the AFM images of glass substrates receiving RIE for 0–3 h. The roughening of glass surfaces by RIE can be confirmed in the images. Figure 3 shows the root mean square (RMS) roughness of textured structures formed on the glass substrates as a function of RIE duration. Although the surface roughness increased monotonically with RIE duration, the surface roughness does not increase in proportion to

the duration but the roughness increase more significantly after 2 h. This might be due to masking effect by deposited material formed during RIE.

~3 μm-thick a-Si films were then deposited by EB evaporation on the textured glass substrates at room temperature, 300 °C, and 500 ºC at a deposition rate of 4.6 nm/s. FLA was performed using a 7-ms-pulse light with fluences of 7–19 J/cm^2 for the samples preheated at 500 °C in Ar atmosphere. Only one pulse was irradiated for each sample. The crystalline fraction and grain size of the Si films after FLA were evaluated by Raman spectroscopy. The surface morphology of Si films was evaluated using an optical microscope and scanning electron microscope (SEM). The formed poly-Si films were also characterized by cross-sectional transmission electron Microscopy (TEM) and electron diffraction (ED) pattern.

3. Results and discussion

Figure 4 shows the Raman spectra of Si films after FLA at a constant fluence of 17.04 J/cm^2 for a-Si films deposited at room temperature on glass substrates receiving RIE with durations of 0–3 h. A peak around 520.5 cm^{-1}, originating from c-Si phase, is seen only when RIE was performed for 2 hours or longer. This indicates that the crystallization of EB-evaporated a-Si films occurs at a lower fluence on a glass surface with more surface roughness. Figure 5 shows the optical reflectance spectra of Si films before FLA formed on glass substrates with textures formed by RIE with various durations. The optical reflectance on the Si films greatly reduces by increasing RIE duration. The crystallization of a-Si films only for the films prepared on longer RIE-treated glass substrates is probably related to the lower optical reflectance and resulting more absorption of FL pulse light in the Si films.

Figure 6 shows the fluence of a FL pulse required for the crystallization of the EB-evaporated a-Si films on the glass substrates with textures formed by RIE for 0–3 h as a function of substrate temperature during the EB evaporation of a-Si films. As the substrate temperature during EB evaporation increases, the fluence required for crystallization tends to increase, independent of the presence or absence of textures on glass substrates. This may be due to the existence of c-Si grains formed during EB evaporation particularly at high substrate temperature, which we confirmed by Raman spectroscopy (not shown here). The pre-existing c-Si grains may influence the mechanism of crystallization and/or reduce the

absorption of FL light due to less absorption coefficient of a-Si than c-Si. It is found that the usage of a-Si films deposited at lower temperature is more proper for the crystallization at lower fluence. We thus used EB-evaporated a-Si films deposited at room temperature in the following experiments.

Figure 7 shows the Raman spectrum of poly-Si films formed from EB-evaporated a-Si films, deposited at room temperature, on the glass substrate receiving RIE for 0–3 h. The poly-Si film formed on a flat glass substrate shows a c-Si peak with a full width at half maximum (FWHM) of 5.2 cm^{-1}. This value is close to that of poly-Si on a glass substrate receiving RIE for 1 h of 5.8 cm^{-1}. This suggests that there is no significant difference in crystal grain size and similar EC occurs for the samples receiving RIE with a duration of ≤1 h. On the other hand, the FWHM values of the c-Si peaks of ≥8 cm^{-1} are obtained for poly-Si films formed on glass substrates receiving RIE for ≥2 h. These FWHM values correspond to a grain size of 10 nm or less, meaning that poly-Si films consisting of nm-order fine grains are formed on textured glass substrates, unlike in the case of the FLA of EB-evaporated a-Si film on flat glass substrates. This fact indicates that the mechanism of crystallization varies depending on the roughness of glass substrates. The formation of textures on a glass surface may lead to the prevention of lateral thermal diffusion and resulting suppression of liquid-phase EC.

Figure 8 shows the optical microscope images of the poly-Si films. A stripe pattern along the EC direction is seen on the surface of the poly-Si film formed on the flat glass substrate. We also see similar surface morphology on the surface of poly-Si formed on glass textured by 1-h RIE (not shown), which is also an indication of the emergence of the same type of EC. On the contrary, the characteristic traces of the lateral crystallization cannot be seen on the surface of the poly-Si film formed on glass textured by 3-h RIE. It should be emphasized that no cracks are seen on the poly-Si surface. The usage of textured glass may contribute to the suppression of the cracking of poly-Si films.

Figure 9 shows the cross-sectional SEM images of Si films before and after FLA on glass substrates receiving RIE for 0 and 3 h. Cracks are seen in poly-Si on a flat glass substrate, as also observed in Fig. 8. We can understand that the film is cracked during the crystallization by FLA since there is no crack in a precursor a-Si. We also see that the cracks penetrate throughout the film. However, cracks are not observed in the poly-Si on the

textured glass. We confirmed that the cracking Si films is suppressed not partly but entirely in the poly-Si on a textured glass substrate.

Figure 10 shows the cross-sectional TEM images of poly-Si films on glass substrates receiving RIE for 0 and 2 h. Laterally elongated crystal grains along crystallization direction can be seen in the poly-Si film formed on a flat glass substrate, resulting from the emergence of EC. The microstructure is completely different in the poly-Si formed on textured glass, showing no specific lateral structures. Figure 11 shows ED patterns obtained from the poly-Si films at the positions indicated as the circles. The poly-Si on a flat glass substrate shows a pattern with high degree of crystallinity. On the contrary, concentric circular patterns are observed in the poly-Si formed on a textured glass substrate, indicating the formation of randomly-oriented fine crystal grains. This means that EC does not occur in a-Si films on highly textured a-Si and uniform solid-phase nucleation dominates the crystallization. The change in the mechanism of the crystallization may result in the suppression of the cracking of poly-Si films.

We have clarified that the cracking of poly-Si films can be suppressed by using textured glass substrates, which will enables us to fabricate thin-film solar cells using the poly-Si films formed from EB-evaporated a-Si films. The textured structure may contribute to light trapping and resulting enhancement in a photocurrent in the solar cells.

4. Conclusions

We confirmed the crystallization of the EB-evaporated a-Si films by FLA on textured glass substrates. The use of a textured glass substrate can reduce the optical reflectance on the surface of a-Si films and reduce the fluence of a FL pulse required for crystallization. We also observed the change in the mechanism of crystallization of EB-evaporated a-Si films depending on the roughness of glass surfaces or a substrate temperature during EB evaporation. The formation of a poly Si film on a textured glass can contribute more photocurrent in a thin film polysilicon solar cell due to less optical reflection and more effective optical trapping.

Acknowledgment

EB-evaporated a-Si films were provided by ULVAC, Inc.

References

1) M. A. Green, Sol. Energy **74**, 181 (2003).
2) W. Fuhs, S. Gall, B. Rau, M. Schmidt, and J. Schneider, Sol. Energy **77**, 961 (2004).
3) M. Spitzer, J. Schewchun, E. S. Vera, and J. J. lofersky, Proc. 14th IEEE PV Specialists Conf., 375 (1980).
4) A. A. D. T. Adikaari, N. K. Mudugamuwa, and S. R. P. Silva, Sol. Energy Mater. Sol. Cells **92**, 634 (2008).
5) J. K. Saha, K. Haruta, M. Yeo, T. Koabayshi, and H. Shirai, Sol. Energy Mater. Sol. Cells **93**, 1154 (2009).
6) T. Matsuyama, M. Tanaka, S. Tsuda, S. Nakano, and Y. Kuwano, Jpn. J. Appl. Phys. **32**, 3720 (1993).
7) M. J. Keevers, T. L. Young, U. Schubert, and M. A. Green, Proc. 22nd European Photovoltaic Solar Energy Conf., 1783 (2007).
8) I. Gordon, L. Carnel, D. Van Gestel, G. Beaucarne, J. Poortmans, L. Pinckney, and A. Mayolet, Proc. 22nd European Photovoltaic Solar Energy Conf., 1993 (2007).
9) S. Arimoto, H. Morikawa, M. Deguchi, Y. Kawama, Y. Matsuno, T. Ishihara, H. Kumabe, and T. Murotani, Proc. 24th IEEE Photovoltaic Specialists Conf., 1311 (1994).
10) K. Ohdaira, S. Nishizaki, Y. Endo, T. Fujiwara, N. Usami, K. Nakajima, and H. Matsumura, Jpn. J. Appl. Phys. **46**, 7198 (2007).
11) K. Ohdaira, T. Fujiwara, Y. Endo, S. Nishizaki, and H. Matsumura, Jpn. J. Appl. Phys. **47**, 8239 (2008).
12) K. Ohdaira, T. Fujiwara, Y. Endo, S. Nishizaki, and H. Matsumura, J. Appl. Phys. **106**, 044907 (2009).
13) K. Ohdaira, Y. Endo, T. Fujiwara, S. Nishizaki, and H. Matsumura, Jpn. J. Appl. Phys. **46**, 7603 (2007).
14) K. Ohdaira, T. Nishikawa, K. Shiba, H. Takemoto, and H. Matsumura, Thin Solid Films **21**, 518 (2007).
15) K. Ohdaira and H. Matsumura, Thin Solid Films **524**, 161 (2012).
16) K. Ohdaira and T. Watanabe, Thin Solid Films **595**, 235 (2015).
17) K. Ohdaira, Thin Solid Films **575**, 21 (2015).

18) K. Ohdaira, T. Fujiwara, Y. Endo, K. Nishioka, and H. Matsumura, J. Cryst. Growth **311**, 769 (2009).
19) K. Ohdaira, T. Nishikawa, and H. Matsumura, J. Cryst. Growth **312**, 2834 (2010).
20) K. Ohdaira, T. Nishikawa, K. Shiba, H. Takemoto, and H Matsumura, Phys. Status Solid C **7**, 604 (2010).
21) K. Ohdaira, H. Takemoto, T. Nishikawa, and H. Matsumura, Curr. Appl. Phys. **10**, 402 (2010).
22) K. Ohdaira, N. Tomura, S. Ishii, and H. Matsumura, Electrochem. Solid-State Lett. **14**, H372 (2011).
23) K. Ohdaira, Can. J. Phys. **92**, 718 (2014).
24) B. Pétz, L. Dobos, D. Panknin, W. Skorupa, C. Lioutas, and N. Vouroutzis, Appl. Surf. Sci. **242**, 185 (2005).
25) F. Terai, S. Matsunaka, A. Tauchi, C. Ichikawa, T. Nagatomo, and T. Homma, J. Electrochem. Soc. **153**, H147 (2006).
26) H. Habuka, A. Hara, T. Karasawa, and M. Yoshioka, Jpn. J. Appl. Phys. **46**, 937 (2007).
27) H.-D. Geiler, E. Glaser, G. Gotz, and M. Wagner, J. Appl. Phys. **59**, 3091 (1986).
28) A. A. Sirenko, J. R. Fox, I. A. Akimov, X. X. Xi, S. Ruvimov, and Z. Liliental-Weber, Solid State Comm. **113**, 553 (2000).
29) M. Yang, D. Huang, P. Hao, F Zhang, X. Hou, and X. Wan, J. Appl. Phys. **75**, 651 (1994).
30) H. Takahashi, H. Nagata, H. Kataoka, and H. Takai, J. Mater. Res. **10**, 2736 (1995).
31) K. Ohdaira, S. Ishii, N. Tomura, and H. Matsumura, J. Nanosci. Nanotechnol. **12**, 591 (2012).
32) K. Kurata and K. Ohdaira, Ext. Abst. 2018 Int. Conf. Solid State Devices and Materials (SSDM2018), 2018, PS-6-16.

Figure Captions

Fig. 1. (Color online) Schematic diagram of EC.

Fig. 2. (Color online) Surface AFM images of glass substrates after RIE for (a) 0 h, (b) 1 h, (c) 2 h, and (d) 3 h.

Fig. 3. RMS roughness of glass surfaces as a function of RIE duration. The error bars in the figure were obtained from three observed positions in two samples.

Fig. 4. Raman spectra of Si films after FLA at a fluence of 17.04 J/cm^2 prepared on glass substrates receiving RIE with durations of 0–3 h.

Fig. 5. Optical reflectance spectra of Si films before FLA on glass substrates with textures formed by RIE with various durations.

Fig. 6. Fluence of a FL pulse required for the crystallization of the EB-evaporated a-Si films on textured glass substrates as a function of substrate temperature during the EB evaporation of a-Si films.

Fig. 7. Raman spectra of poly-Si films after FLA on glass substrates receiving RIE with various durations.

Fig. 8. (Color online) Optical microscope images of poly-Si film surfaces formed on (a) flat and (b) textured glass substrates by 3-h RIE.

Fig. 9. Cross-sectional SEM images of Si films before and after FLA formed on flat and textured glass substrates by 3-h RIE: (a) flat, before FLA, (b) flat, after FLA, (c) textured, before FLA, (d) textured, after FLA.

Fig. 10. Cross-sectional TEM images of poly-Si films formed on glass substrates receiving RIE for (a) 0 h and (b)2 h. ED patterns were measured at the points indicated as the red circles.

Fig. 11. ED patterns of poly-Si films formed on glass substrates receiving RIE for (a) 0 h and (b)2 h.

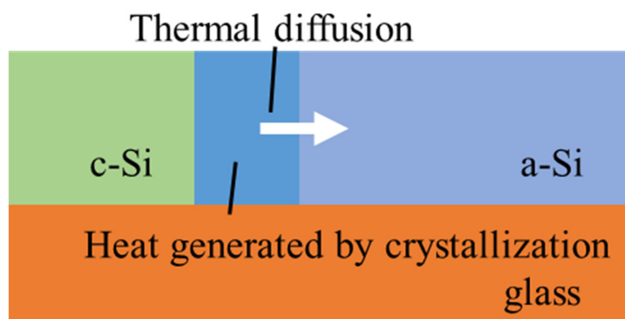

Fig. 1. (Color Online) K. Kurata *et al*.

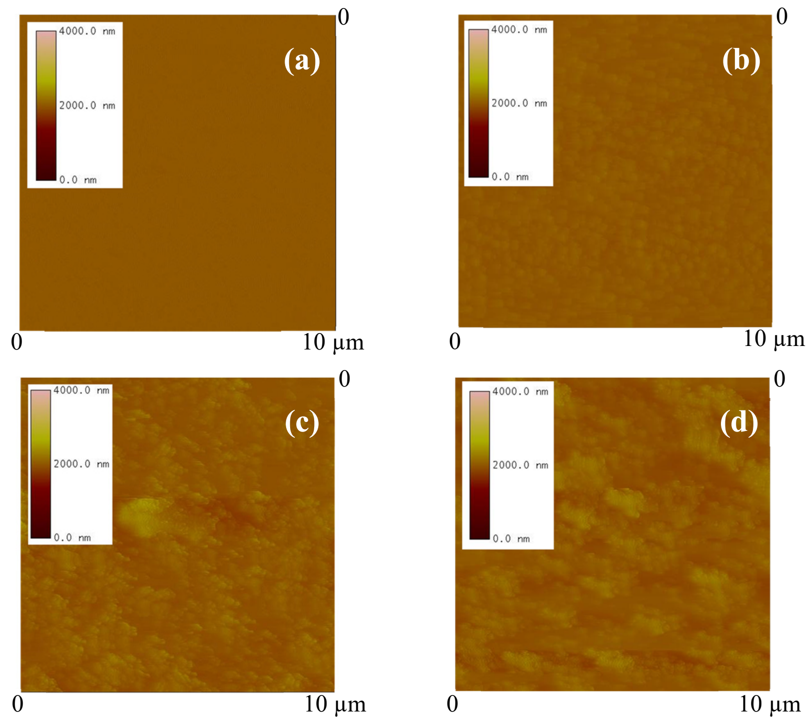

Fig. 2. (Color Online) K. Kurata *et al*.

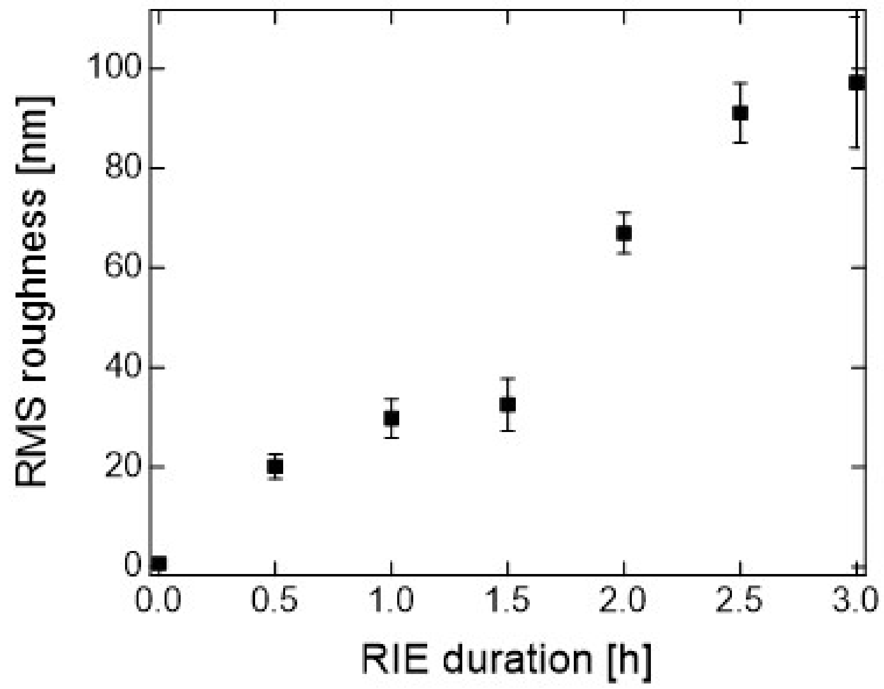

Fig. 3. (Color Online) K. Kurata *et al*.

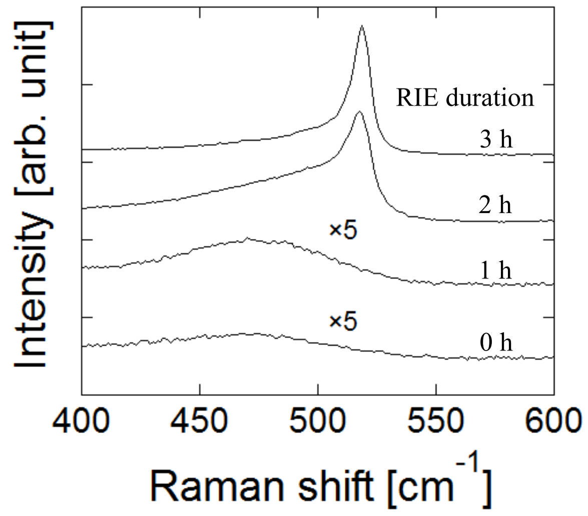

Fig. 4. K. Kurata *et al*.

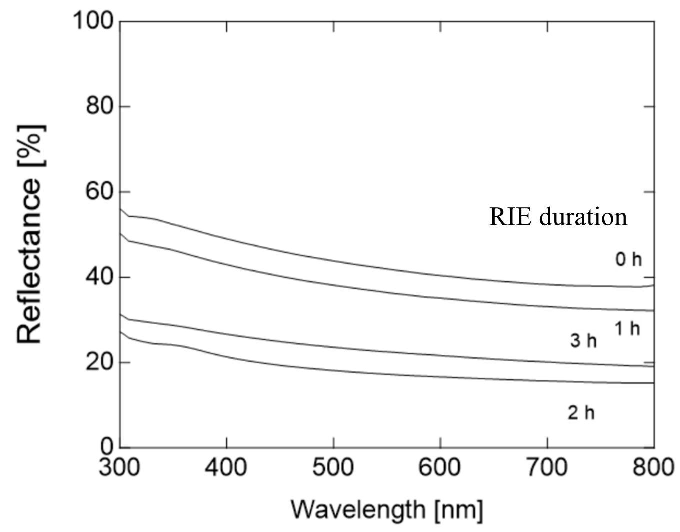

Fig. 5. K. Kurata *et al*.

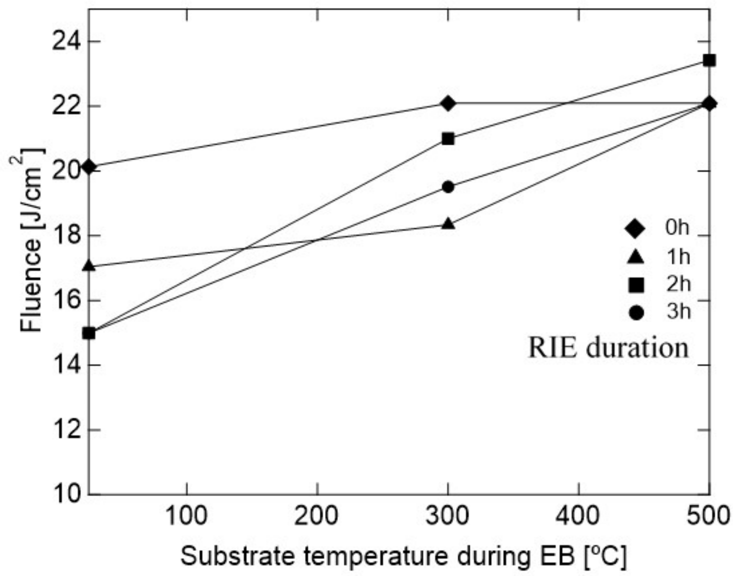

Fig. 6. K. Kurata *et al*.

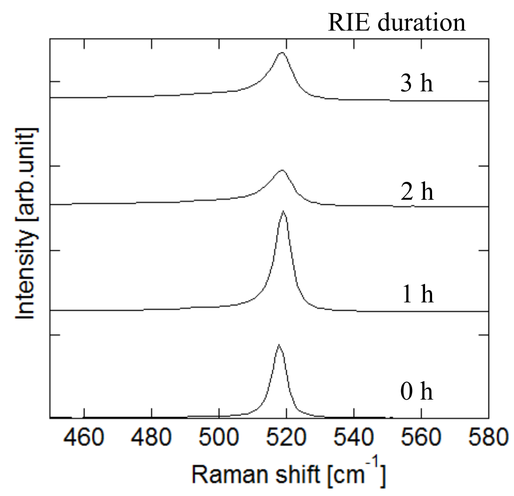

Fig. 7. K. Kurata *et al*.

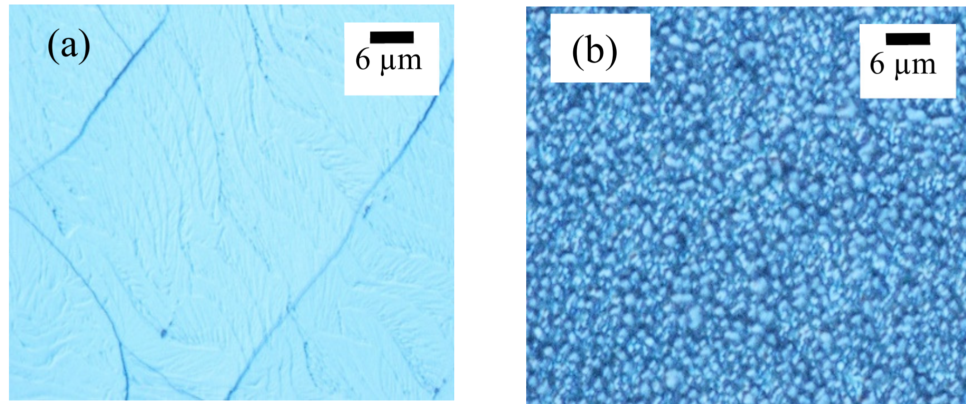

Fig. 8. (Color Online) K. Kurata *et al*.

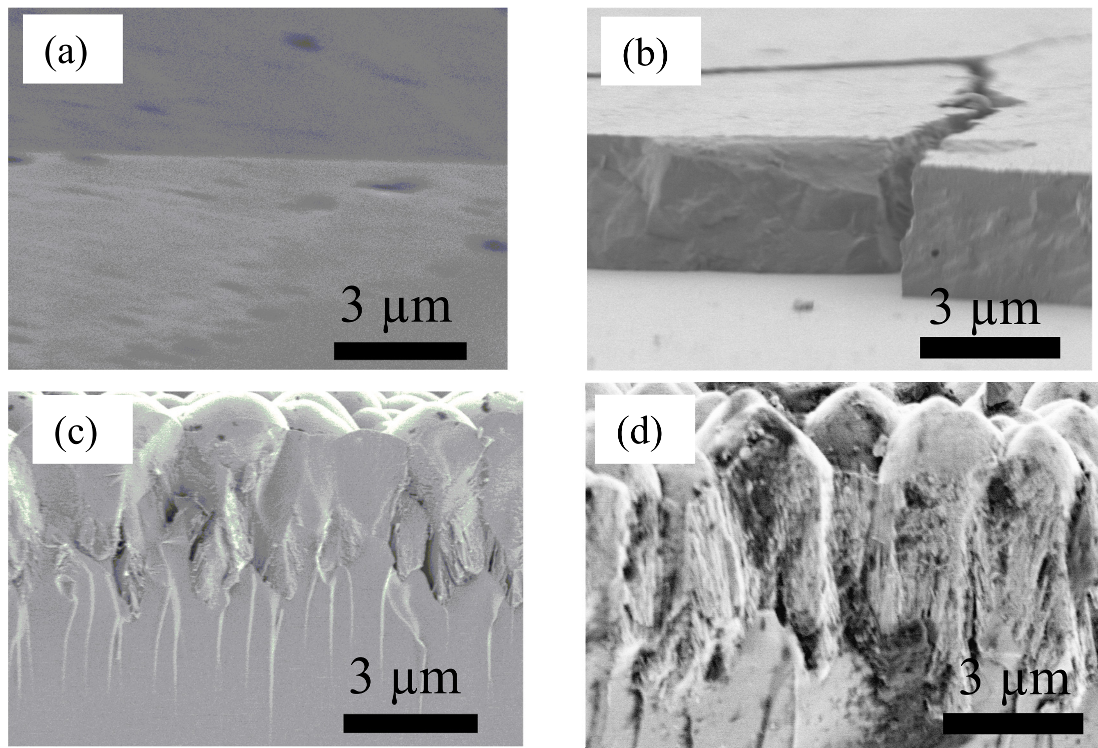

Fig. 9. (Color Online) K. Kurata *et al*.

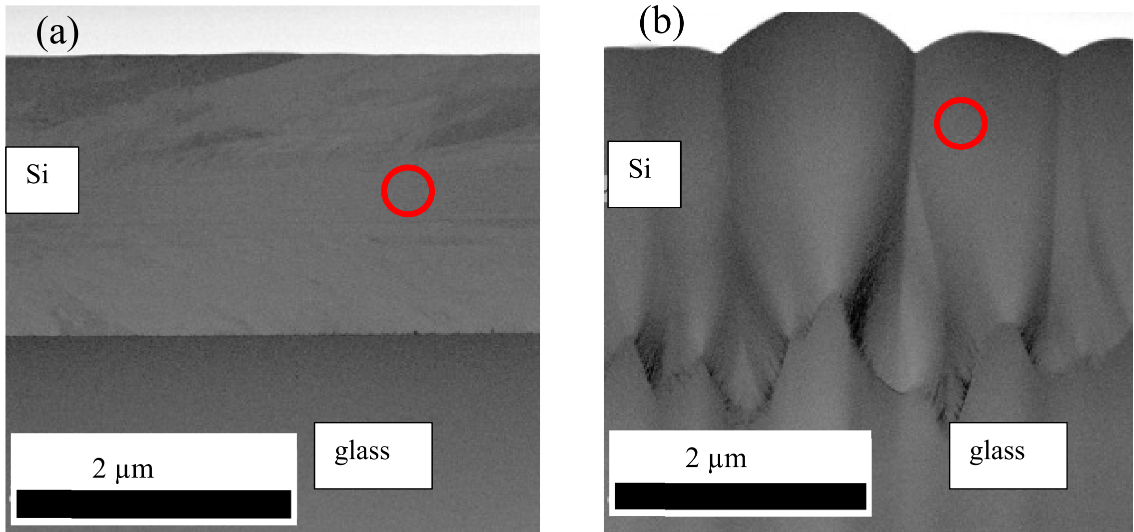

Fig. 10. (Color Online) K. Kurata *et al*.

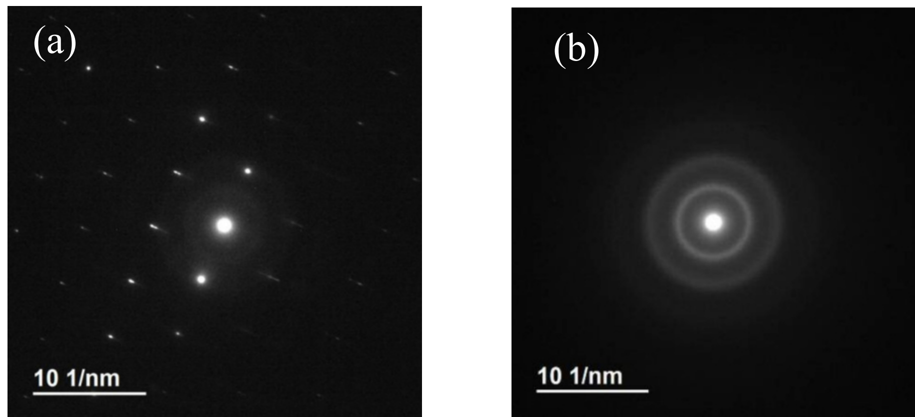

Fig. 11. (Color Online) K. Kurata *et al*.